Specific absorption rate monitor for in-vivo parallel transmission at 7 Tesla

M. A. Cloos[1], N. Boulant[1], M. Luong[2], G. Ferrand[2], D. Le Bihan[1], and A. Amadon[1]
[1]CEA, DSV, I2BM, NeuroSpin, LRMN, Gif-sur-Yvette, France, [2]CEA, DSM, IRFU, SACM, Gif-sur-Yvette, France

Introduction:

When using a transmit array at high field, it is well established that high local specific absorption rate (SAR) values can occur [1]. In order to guarantee patient safety without harsh limitations to in-vivo transmit-SENSE [2] applications, subtle SAR monitoring is therefore necessary. In the recent past, a comprehensive solution involving pre-calculated B1-field-maps and local pickup-coils was demonstrated at 3 Tesla [3]. In this work, we report the implementation of a similar design at 7 Tesla, this time based on the real-time measurement of the individual power outputs of the RF amplifiers, combined with pre-calculated simulations over a variety of human head models and positions.

Methods:

In a preliminary step, the Finite Element Method electromagnetic simulations (HFSS, Ansoft, Pittsburgh, PA) were validated by comparing simulated and measured B1 maps [4] in a phantom with known dielectric and conductive properties [5], using respectively a modelled and actual 8-dipole home-made RF coil (Fig. 1). Experimental verification was performed on a Siemens 7T Magnetom scanner (Erlangen, Germany) equipped with an 8-channel transmit array. Subsequently, simulations were performed on several head models (Aarkid, East Lothian, Scotland, and Virtual Family [6]) in various positions in the coil. Individual E-field maps were then extracted and exported for later SAR assessment on the scanner console. There, once a transmit-SENSE RF pulse is designed, it is loaded in our dedicated SAR-Assessment Software (SAS). Meanwhile, the power out of the amplifiers is measured through the use of directional couplers with power meters (TALES, Siemens). Because the phases out of the amplifiers are not monitored yet, the absolute values of the E-fields coming from the different transmit channels are summed in our SAS, thereby assuming worst-case constructive interference everywhere in the head. The 10-gram average SAR is then computed using a cubic region-growth algorithm. A second safety layer then consists of taking the worst 10-gram SAR found over all the different head models (Fig. 2). Our SAS was implemented in C++/CUDA™, allowing designed pulses to be analyzed in real-time using GPUs (NVIDIA®). Once the worst peak SAR value is recorded, a maximum RF pulse duty-cycle is derived based on the IEC guidelines (10 W/kg in any 10-gram cell of the head). Likewise, individual power levels are returned which determine thresholds to be set on the power meters, by integrating predetermined calibration factors and a margin of measurement error. If the power exceeds any one of the 8 thresholds, the acquisition is automatically stopped, while if it is significantly lower, our method ensures that the resulting SAR can only be less than the one assessed. To test the software and obtain the appropriate calibration factors, the calculated power levels were compared with measurements for a number of pulse sequences. Results were compared with similar power measurements performed replacing the coil with 50-Ohm terminators.

Results & discussion:

Simulated and measured B1-maps in the phantom were compared (Fig. 3) for each of the individual transmit-channels, resulting in correlation factors well above 0.95 for all except the two channels near the aperture (Fig 1). The reduced correlation of 0.91 in this case could come from a combination of the glass part of the bottleneck (Fig. 1) and gradient RF shielding, not included in the simulations. Power measurements with the loaded coil revealed a maximum increase of up to 20% compared to the theoretical integrated powers. Obtained relative deviations remained constant between different measurements and showed good correlation with results obtained using 50-Ohm terminators. This small discrepancy between calculated and measured power was included in the calibration factor, effectively adding a safety margin to account for measurement errors and uncertainties in simulations. Currently, scaling factors based on patient's weight are incorporated in the SAS. But simulations indicate that for this particular coil, the local SAR could increase with larger head sizes. Later versions of the SAS could possibly use patient weight to include or exclude certain head models. Based on the three head-models currently included in the SAS, reasonable maximum duty-cycles were found for various pulse sequences (Table).

Conclusions:

Using the power monitors available on each of the individual transmit channels, a practical SAR monitoring system is suggested for use with in-vivo transmit-SENSE applications. It relies on a collection of head models whose E-maps were pre-calculated for rapid assessment of the worst-case highest local SAR. Because of its conservative approach, it thus avoids having to worry about the particular head morphology of every subject to be scanned. Experience will tell whether large power level variations occur across head models and pulses.

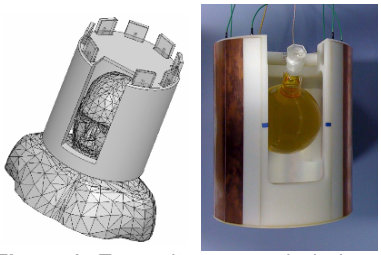

Figure 1: Transmit array made in house and used for this work. Left) coil model used for simulations, showing one of the head models.

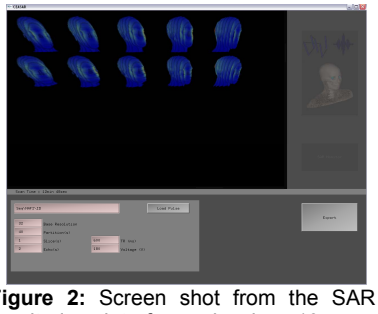

Figure 2: Screen shot from the SAR monitoring interface showing 10-gram Local SAR distributions for a given pulse and sequence. The user interface allows sequence parameters to be modified within SAR guidelines.

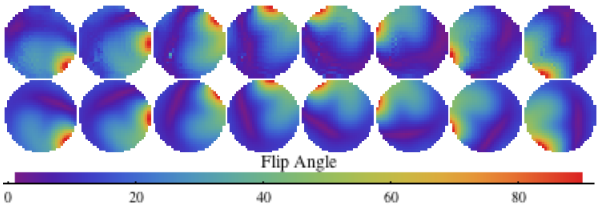

Figure 3: Experimental (top) and simulated (bottom) B1-maps showing the axial slices trough the center of the phantom for each of the 8 transmit channels.

Table 1

Sequence	Pulse duration	Minimum TR
AFI CP-mode	0.75 ms square	284 ms
AFI 5-spokes (20°)	3.5 ms	22 ms
AFI K_t-points (15°)	0.95 ms	55 ms
GRE K_t-points (15°)	0.95 ms	28 ms

References:
[1]Collins CM, et al., ISMRM 15:1092 (2007) [2] Katscher U., et al., MRM 49:144-150 (2002) [3] Graesslin I. et al., ISMRM 17:302 (2009)
[4] Yarnykh V., et al., MRM 57:192-200 (2007) [5] Fukunaga K., et al., IEEE ICDL:425-428 (2005) [6] Christ, A., et al., *'Virtual Family'* ACES (2007)